

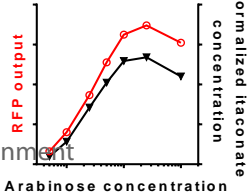
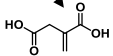
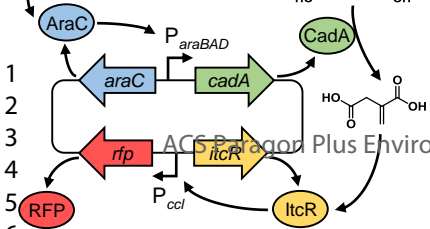
This document is confidential and is proprietary to the American Chemical Society and its authors. Do not copy or disclose without written permission. If you have received this item in error, notify the sender and delete all copies.

## **A transcription factor-based biosensor for detection of itaconic acid**

Journal:	<i>ACS Synthetic Biology</i>
Manuscript ID	sb-2018-000576.R2
Manuscript Type:	Article
Date Submitted by the Author:	n/a
Complete List of Authors:	Hanko, Erik; University of Nottingham Minton, Nigel; University of Nottingham, Synthetic Biology Research Centre Malys, Naglis; University of Nottingham, School of Life Sciences

SCHOLARONE™  
Manuscripts

# ACS Synthetic Biology



1  
2  
3  
4  
5  
6

1  
2  
3 **1 A transcription factor-based biosensor for detection of itaconic acid**  
4  
5

6 2

7  
8 3 Erik K. R. Hanco<sup>1</sup>, Nigel P. Minton<sup>1</sup> and Naglis Malys<sup>1\*</sup>  
9

10 4

11  
12 5 <sup>1</sup>BBSRC/EPSRC Synthetic Biology Research Centre (SBRC), School of Life Sciences, Centre for  
13

14 6 Biomolecular Sciences, The University of Nottingham, Nottingham, NG7 2RD, United Kingdom  
15

16 7

17  
18 8 \*Author to whom correspondence should be addressed; E-Mail: naglis.malys@nottingham.ac.uk  
19

20 9  
21  
22  
23  
24  
25  
26  
27  
28  
29  
30  
31  
32  
33  
34  
35  
36  
37  
38  
39  
40  
41  
42  
43  
44  
45  
46  
47  
48  
49  
50  
51  
52  
53  
54  
55  
56  
57  
58  
59  
60

## 1 Abstract

2 Itaconic acid is an important platform chemical that can easily be incorporated into polymers and  
3 has the potential to replace petrochemical-based acrylic or methacrylic acid. A number of  
4 microorganisms have been developed for the biosynthesis of itaconate including *Aspergillus terreus*,  
5 *Escherichia coli* and *Saccharomyces cerevisiae*. However, the number of strains and conditions that  
6 can be tested for increased itaconate titers are currently limited due to the lack of high-throughput  
7 screening methods. Here we identified itaconate-inducible promoters and their corresponding LysR-  
8 type transcriptional regulators from *Yersinia pseudotuberculosis* and *Pseudomonas aeruginosa*. We  
9 show that the *YpltcR/P<sub>ccI</sub>* inducible system is highly inducible by itaconic acid in the model  
10 gammaproteobacterium *E. coli* and the betaproteobacterium *Cupriavidus necator* (215- and 105-  
11 fold, respectively). The kinetics and dynamics of the *YpltcR/P<sub>ccI</sub>* inducible system are investigated and  
12 we demonstrate, that in addition to itaconate, the genetically encoded biosensor is capable of  
13 detecting mesaconate, *cis*-, and *trans*-aconitate in a dose-dependent manner. Moreover, the  
14 fluorescence-based biosensor is applied in *E. coli* to identify the optimum expression level of *cadA*,  
15 the product of which catalyzes the conversion of *cis*-aconitate into itaconate. The fluorescence  
16 output is shown to correlate well with itaconate concentrations quantified using high-performance  
17 liquid chromatography coupled with ultraviolet spectroscopy. This work highlights the potential of  
18 the *YpltcR/P<sub>ccI</sub>* inducible system to be applied as biosensor for high-throughput microbial strain  
19 development to facilitate improved itaconate biosynthesis.

20 **Keywords:** itaconic acid, inducible gene expression, fluorescence-based biosensor, *Yersinia*  
21 *pseudotuberculosis*, *Pseudomonas aeruginosa*, macrophage infection

1  
2  
3 1 The use of biological processes for the production of chemicals and fuels is a promising alternative to  
4  
5 2 the traditional approach of chemical manufacture.<sup>1</sup> They offer the opportunity to convert renewable  
6  
7 3 or waste feedstocks into higher value compounds of industrial interest.<sup>2</sup> Although many biological  
8  
9 4 processes have the potential to replace synthetic chemistry, product titers and productivity often  
10  
11 5 remain to be optimized in order to achieve economically competitive conversion rates.<sup>1, 3</sup> To  
12  
13 6 facilitate and expedite the implementation of biocatalysts with improved performance, low-cost and  
14  
15 7 high-throughput microbial engineering strategies need to be developed.

17 8 Itaconic acid is an attractive platform chemical with a wide range of industrial applications,  
18  
19 9 such as in rubber, detergents, or surface active agents.<sup>4</sup> In 2004, it was reported by the US  
20  
21 10 Department of Energy to be one of the top twelve building block chemicals from biomass.<sup>5</sup> The C5-  
22  
23 11 dicarboxylic acid can be converted into poly(acrylamide-co-itaconic acid) which is used as a  
24  
25 12 superabsorbent for aqueous solutions, or poly(methyl methacrylate), also known as Plexiglas.<sup>6</sup>

28 13 Itaconate is a naturally occurring metabolite formed by decarboxylation of aconitate, an  
29  
30 14 intermediate of the citric acid cycle. A number of microorganisms, including *Aspergillus terreus*,<sup>7</sup>  
31  
32 15 *Ustilago maydis* (also known as *U. zeae*)<sup>8</sup> and *Candida sp.*,<sup>9</sup> have been described as natural producers  
33  
34 16 of itaconic acid. It is also produced as an antimicrobial compound by macrophages, mammalian  
35  
36 17 immune cells.<sup>10, 11</sup> In *A. terreus* and macrophages, itaconate is synthesized from the tricarboxylic acid  
37  
38 18 cycle intermediate *cis*-aconitate through the action of a *cis*-aconitate decarboxylase (CadA). In  
39  
40 19 contrast, in *U. maydis* it is produced *via* the unusual intermediate *trans*-aconitate.<sup>12</sup> Heterologous  
41  
42 20 expression of the *A. terreus cadA* gene has demonstrated that the biosynthesis of itaconic acid can  
43  
44 21 be achieved in different host organisms than the natural producer.<sup>13</sup> So far, the highest titer of  
45  
46 22 biotechnologically produced itaconate has been obtained by fermentation of *A. terreus*.<sup>14-16</sup>  
47  
48 23 However, due to feedback inhibition of itaconate biosynthesis at higher concentrations,<sup>17</sup>  
49  
50 24 considerable research efforts have been directed towards developing alternative microbial  
51  
52 25 biocatalysts. Other microorganisms that have been investigated for the biosynthesis of itaconic acid  
53  
54 26 include *Pseudozyma antarctica*, *Corynebacterium glutamicum*, *Escherichia coli*, *Saccharomyces*

1  
2  
3 1 *cerevisiae*, *Yarrowia lipolytica* and species of *Candida* and *Ustilago*.<sup>9, 18-24</sup> Although some of these  
4  
5 2 microorganisms exhibit beneficial traits, such as a high tolerance to itaconate and a low pH,<sup>19, 22</sup>  
6  
7 3 production titers need to be considerably improved.

8  
9 4 Genetically encoded biosensors have gained increasing interest as molecular tools enabling  
10  
11 5 high-throughput strain development.<sup>25</sup> They are composed of transcription-based inducible gene  
12  
13 6 expression systems linked to a reporter or an antibiotic resistance gene.<sup>26, 27</sup> By using a fluorescent  
14  
15 7 reporter gene, changes in intracellular metabolite concentrations can easily be monitored by a  
16  
17 8 fluorescence output enabling the screen of millions of single-cells in a rapid manner.<sup>25</sup> Biosensors  
18  
19 9 have been successfully applied to increase products titers of platform chemicals such as acrylate, 3-  
20  
21 10 hydroxypropionate (3-HP) and glucarate.<sup>26, 28</sup> To date, no itaconate biosensor has been developed  
22  
23 11 which could facilitate the screening process for both metabolically engineered strains and  
24  
25 12 alternative feedstocks, such as biomass hydrolysates, to improve yields and decrease production  
26  
27 13 costs.<sup>29</sup>

28  
29  
30 14 This study was aimed to identify an itaconate-inducible gene expression system and  
31  
32 15 construct a fluorescence-based biosensor. Several natural compounds were screened for biosensor  
33  
34 16 induction and induction kinetics measured. Moreover, the developed biosensor was exploited in the  
35  
36 17 optimization of itaconate production in *E. coli* and its output compared to analytically determined  
37  
38 18 itaconate titers.

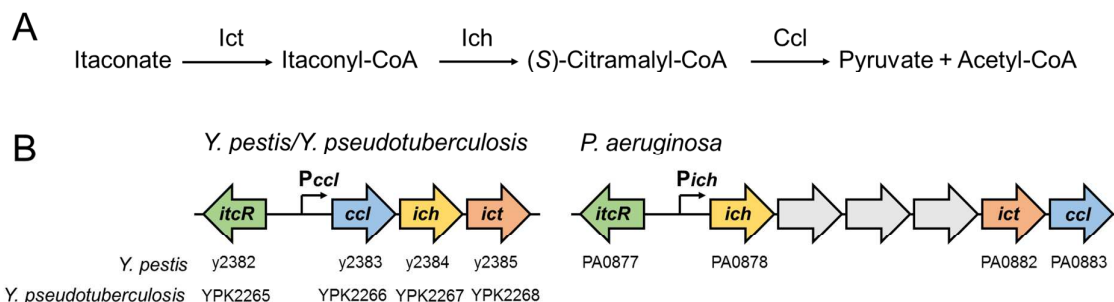
39  
40  
41 19  
42  
43  
44  
45  
46  
47  
48  
49  
50  
51  
52  
53  
54  
55  
56  
57  
58  
59  
60

## 1 Results and Discussion

### 2 Identification of an itaconic acid-inducible system

3 To build an itaconate biosensor, which can be applied across different species, both elements of a  
4 transcription-based inducible system, a transcriptional regulator (TR) and the corresponding  
5 inducible promoter, are needed. Bacterial degradation pathways, which are often activated  
6 exclusively in the presence of the compound to be degraded, represent a rich source of inducible  
7 promoters. Even though the pathway for itaconate catabolism had been known for more than 50  
8 years,<sup>30</sup> and a few bacteria including *Pseudomonas* spp., *Salmonella* spp., and *Micrococcus* sp. have  
9 been shown to possess enzymatic activities for itaconate degradation,<sup>31</sup> the genes encoding these  
10 enzymes have only recently been identified in *Yersinia pestis* and *Pseudomonas aeruginosa*.<sup>32</sup> The  
11 pathway comprises three enzymatic reactions (Figure 1A). The first reaction is catalyzed by itaconate  
12 CoA transferase (Ict) which converts itaconate to itaconyl-CoA. The CoA ester is subsequently  
13 hydrated to (S)-citramalyl-CoA by itaconyl-CoA hydratase (Ich) which is then cleaved into acetyl-CoA  
14 and pyruvate by (S)-citramalyl-CoA lyase (Ccl). The production of the Ict and Ich homologs (RipA and  
15 RipB, respectively) by *Salmonella enterica* was shown to be strongly induced after macrophage  
16 infection.<sup>33</sup> The upregulation of *ripA* and *ripB* was suggested by Sasikaran and coworkers to result  
17 from macrophagic itaconate secretion as part of the defence mechanism against pathogenic  
18 bacteria.<sup>32, 34</sup> Most likely, the promoters of the gene clusters encoding the enzymes for itaconate  
19 catabolism in *Y. pestis* and *P. aeruginosa* harbor regulatory elements required for transcription of  
20 these genes in the presence of itaconate. Interestingly, a gene encoding a LysR-type transcriptional  
21 regulator (LTTR, here termed ItcR) is located in the opposite direction of both the *Y. pestis* *ccl-ich-ict*  
22 operon (also referred to as *ripABC* operon) and the *P. aeruginosa* putative six-gene operon encoding  
23 Ich, Ict, Ccl, and three other proteins (Figure 1B). The genes coding for LTTRs are occasionally  
24 transcribed in divergent orientation with respect to the cluster of genes they regulate,<sup>35</sup> which led to  
25 the hypothesis that transcription of the *Y. pestis* and *P. aeruginosa* itaconate degradation pathway

1 genes is mediated by their corresponding divergently oriented LTTR genes from an inducible  
 2 promoter located in their intergenic regions.



3  
 4 **Figure 1.** Bacterial itaconate degradation pathway. (A) The enzymes involved in bacterial itaconate  
 5 degradation include: itaconate CoA transferase (Ict), itaconyl-CoA hydratase (Ich), (S)-citramalyl-CoA  
 6 lyase (Ccl). (B) The gene clusters in *Y. pestis*, *Y. pseudotuberculosis* and *P. aeruginosa* encoding the  
 7 enzymes required for itaconate catabolism. Divergently oriented LTTR genes (*itcR*) and putative  
 8 itaconate-inducible promoters are depicted. Gene names and locus tags are shown under schematic  
 9 illustration of each gene cluster.

### 10 Itaconic acid-inducible gene expression is mediated by a LysR-type transcriptional 11 regulator

12 To test our hypothesis that itaconate degradation pathway is controlled by the transcriptional  
 13 regulator and corresponding inducible promoter, we cloned both the *P. aeruginosa* PAO1 and the  
 14 *Yersinia pseudotuberculosis* YPIII DNA fragments with putative itaconate-inducible system,  
 15 containing intergenic region with promoters  $P_{ich}$  and  $P_{ccl}$ , respectively, and gene of the transcriptional  
 16 regulator (*itcR*) (Figure 1B), into the reporter plasmid pEH006. The latter plasmid has previously been  
 17 demonstrated to be suitable for the analysis of inducible systems (Table 1).<sup>36</sup> The nucleotide  
 18 sequence of the *Y. pseudotuberculosis* itaconate-inducible system is identical to the *Y. pestis* one,  
 19 except for three single nucleotide polymorphisms in *ItcR* coding sequence (YPK\_2265) resulting in  
 20 one amino acid difference. The nucleotide sequences of the intergenic regions containing putative

1 itaconate-inducible promoters are provided in Figure S1. To investigate the potential applicability of  
 2 the two putative itaconate-inducible systems across different species, red fluorescent protein (RFP)  
 3 reporter gene expression in response to itaconate was measured by fluorescence output in the  
 4 model gammaproteobacterium *E. coli* MG1655 and the betaproteobacterium *Cupriavidus necator*  
 5 H16. The latter is a model chemolithoautotroph with the ability to produce energy and chemicals  
 6 from carbon dioxide and is therefore of interest in biotechnological applications. Single time point  
 7 fluorescence measurements for *E. coli* and *C. necator* harboring the putative itaconate-inducible  
 8 systems, composed of transcriptional regulator and inducible promoter (ItcR/P), were performed in  
 9 the absence and presence of itaconate (Figure 2). In both microorganisms, reporter gene expression  
 10 from the *Y. pseudotuberculosis* (*Yp*) inducible system (pEH086) is induced significantly ( $p < 0.01$ ) six  
 11 hours after supplementation with 5 mM itaconate (215-fold in *E. coli* and 105-fold in *C. necator*,  
 12 Figure 2A and 2B, respectively). In contrast, the *P. aeruginosa* (*Pa*) inducible system *P<sub>altcR</sub>/P<sub>ich</sub>*  
 13 (pEH177) does not mediate reporter gene expression in response to itaconate in *E. coli*, whereas in  
 14 *C. necator* it demonstrates an 18.5-fold induction. In comparison, in *E. coli* MG1655, the level of  
 15 induction mediated by the *Y. pseudotuberculosis* itaconate-inducible system is considerably higher  
 16 than the commonly used L-arabinose-inducible system which is subject to catabolite repression. A  
 17 culture of *E. coli* MG1655 harboring pEH006 demonstrated a 39-fold increase in RFP expression six  
 18 hours after addition of L-arabinose to a final concentration of 0.1% (w/v) in minimal medium.

19

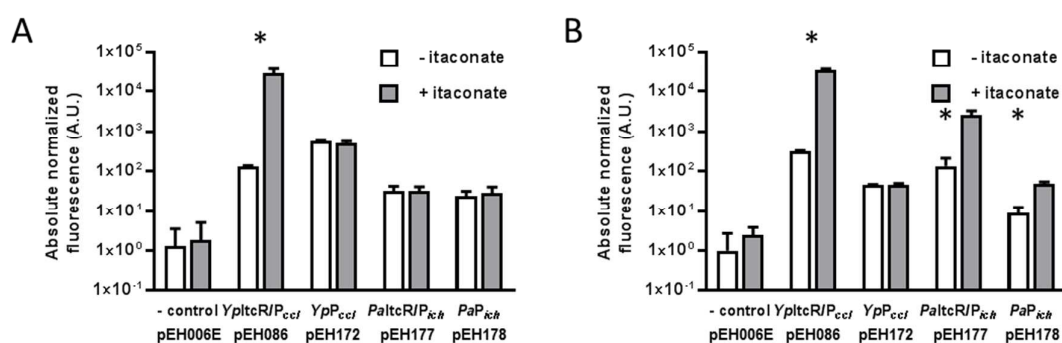
20 **Table 1.** Plasmids used and generated in this study.

Plasmid	Characteristic	Reference or source
pBBR1MCS-2-PphaC-eyfp-c1	Kan <sup>r</sup> ; broad host range vector used to amplify the origin of replication	<sup>37</sup>
pEH006	Cm <sup>r</sup> ; modular vector for the evaluation of inducible systems; <i>P<sub>araC</sub>-araC-T<sub>rrnB1</sub></i> and <i>P<sub>araBAD</sub>-T7sl-EcRBS-rfp-T<sub>dbl</sub></i>	<sup>36</sup>
pEH006E	Cm <sup>r</sup> ; promoterless pEH006	<sup>36</sup>
pEH086	Cm <sup>r</sup> ; <i>P<sub>itcR</sub>-itcR-T<sub>rrnB1</sub></i> and <i>P<sub>ccl</sub>-rfp-T<sub>dbl</sub></i> from <i>Y. pseudotuberculosis</i> YPIII genomic DNA	This study
pEH164	Cm <sup>r</sup> ; <i>P<sub>araC</sub>-araC-T<sub>dbl</sub></i> , <i>P<sub>araBAD</sub>-T7sl-EcRBS-T<sub>rrnB2</sub></i> , <i>YpP<sub>itcR</sub>-YpitcR-T<sub>rrnB1</sub></i> and <i>YpP<sub>ccl</sub>-rfp-</i>	This study

	$T_{dbl}$	
pEH165	$Cm^r$ ; $P_{araC-araC-T_{dbl}}$ , $P_{araBAD-T7sl-EcRBS-cadA-T_{rrnB2}}$ , $YpP_{itcR-YpitcR-T_{rrnB1}}$ and $YpP_{ccf-rfp-T_{dbl}}$	This study
pEH172	$Cm^r$ ; $P_{ccf-rfp-T_{dbl}}$ from <i>Y. pseudotuberculosis</i> YPIII genomic DNA	This study
pEH177	$Cm^r$ ; $P_{itcR-itcR-T_{rrnB1}}$ and $P_{ich-rfp-T_{dbl}}$ from <i>P. aeruginosa</i> PAO1 genomic DNA	This study
pEH178	$Cm^r$ ; $P_{ich-rfp-T_{dbl}}$ from <i>P. aeruginosa</i> PAO1 genomic DNA	This study

1

2



3

**Figure 2.** Influence of ItcR on inducible gene expression. Absolute normalized fluorescence (in arbitrary units) of (A) *E. coli* MG1655 and (B) *C. necator* H16 harboring the *Y. pseudotuberculosis* (*Yp*) and *P. aeruginosa* (*Pa*) itaconate-inducible systems composed of promoter and transcriptional regulator (ItcR/P), and promoter-only (P) implementation in the absence and presence of 5 mM itaconate. Single time point fluorescence measurements were taken six hours after inducer addition. The promoterless reporter plasmid pEH006E was employed as negative control. Error bars represent standard deviations of three biological replicates. Asterisks indicate statistically significant induction values for  $p < 0.01$  (unpaired *t* test).

12

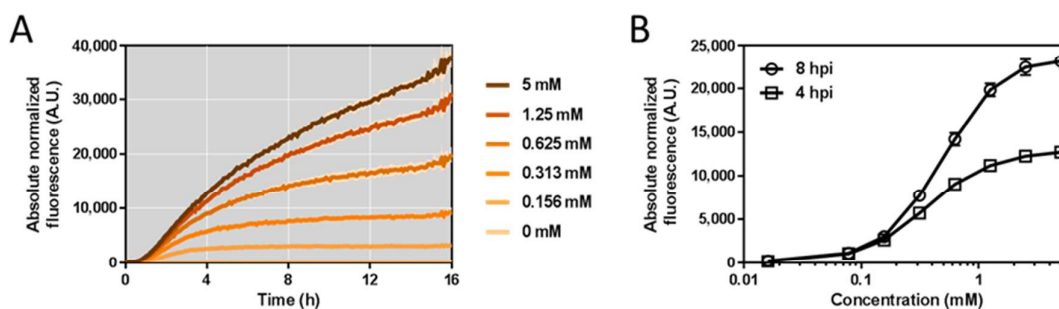
To confirm that itaconate-inducible reporter gene expression is indeed controlled by the episomally encoded ItcR, their coding sequences were removed from the vectors containing  $YpltcR/P_{ccf}$  and  $PaltcR/P_{ich}$ . Single time point fluorescence measurements were repeated for *E. coli* and *C. necator* solely harboring the itaconate-inducible promoters in the absence and presence of

1 itaconate (Figure 2). Without *YpItcR*, induction of reporter gene expression from the *Y.*  
2 *pseudotuberculosis* itaconate-inducible promoter (*YpP<sub>cch</sub>*, pEH172) is abolished in both  
3 microorganisms. This confirms that transcription of the *Y. pseudotuberculosis* itaconate degradation  
4 pathway genes is mediated by their divergently oriented *itcR* gene and that neither of the two tested  
5 microorganisms encodes cross-activating TR homologs. In *E. coli*, the level of normalized  
6 fluorescence from *PaP<sub>ich</sub>* (pEH178) and *PaltrC/P<sub>ich</sub>* (pEH177) is higher than the negative control,  
7 indicating that the promoter itself is active. However, the normalized fluorescence levels are of  
8 equal height, suggesting that the TR might not be produced or able to interact with its cognate  
9 operator sequence to activate gene expression in the presence of the effector. Interestingly, in *C.*  
10 *necator*, even though the coding sequence of *PaltrC* was removed from the plasmid, reporter gene  
11 expression from *PaP<sub>ich</sub>* (pEH178) is induced significantly ( $p < 0.01$ ) after addition of itaconate. A *PaltrC*  
12 homology search in *C. necator* revealed the presence of several chromosomally encoded LTTRs  
13 exhibiting 40-50% protein sequence identity (96-98% coverage). One of the LTTR genes is located  
14 within close proximity to the cluster that includes genes potentially involved in itaconate  
15 degradation similar to *P. aeruginosa* (Figure S2). *C. necator* ItcR homologs can potentially activate  
16 gene expression from the heterologous *P. aeruginosa* itaconate-inducible promoter even in the  
17 absence of its corresponding LTTR. However, since both the induction level, and the absolute  
18 normalized fluorescence in the presence of itaconate, are higher in the plasmid carrying *PaltrC/P<sub>ich</sub>*  
19 (pEH177) than the one carrying *PaP<sub>ich</sub>* (pEH178) alone (by 3.5- and 52-fold, respectively), it can be  
20 concluded that *PaltrC* is involved in activation of gene expression of the itaconate degradation  
21 cluster of genes in *P. aeruginosa* and therefore enables persistence in macrophages. The finding that  
22 expression of the genes encoding enzymes involved in itaconate catabolism is mediated by their  
23 divergently oriented LTTR genes may aid in developing new antimicrobial agents.

## 1 Sensor characterization

2 Due to its functionality in both tested microorganisms, regulator-dependent orthogonality and high  
 3 level of induction, the itaconate-inducible system from *Y. pseudotuberculosis* was selected to be  
 4 further characterized. The sensor was evaluated for its kinetics – the time that is required for the  
 5 system to respond to a change in itaconate levels; dynamics – the range of inducer concentration  
 6 that mediates a linear fluorescence output; and inducer-dependent orthogonality – the specificity  
 7 towards itaconate.

8 *E. coli* MG1655 was transformed with the plasmid harboring the  $YpItcR/P_{ccl}$  inducible system  
 9 (pEH086), cultivated in M9 minimal medium, and fluorescence output was monitored over time  
 10 after supplementation with different concentrations of itaconate. As can be seen from the  
 11 fluorescence curve of induction kinetics, reporter gene expression is activated immediately after  
 12 inducer addition, taking into account the time that is required for RFP maturation (Figure 3A).<sup>38</sup> This  
 13 immediate response suggests, that the system is solely controlled by ItcR and that it is not affected  
 14 by host-originating TRs. Furthermore, it suggests that itaconate is a primary inducing molecule,  
 15 which starts instantly to be uptaken by or diffused into the *E. coli* cells in minimal medium. It should  
 16 be noted that the growth was similar for all itaconate concentrations tested.



17  
 18 **Figure 3.** Kinetics and dynamics of the  $YpItcR/P_{ccl}$  inducible system. (A) Absolute normalized  
 19 fluorescence of *E. coli* MG1655 harboring the  $YpItcR/P_{ccl}$  inducible system (pEH086) in response to  
 20 different concentrations of itaconate added at time zero. The standard deviation of three biological  
 21 replicates is shown as lighter colour ribbon displayed lengthwise the induction kinetics curve. For the

1  
2  
3 1 lower concentrations, the standard deviation is too small to be visible. (B) Dose response curve of  
4  
5 2 the *YpItcR/P<sub>ccI</sub>* inducible system in *E. coli* MG1655, illustrating the correlation between inducer  
6  
7 3 concentration and fluorescence output four and eight hours post induction (hpi) with itaconate.  
8  
9 4 Error bars represent standard deviations of three biological replicates.

10  
11  
12 5  
13  
14 6 The correlation between extracellular inducer concentration and fluorescence output, four  
15  
16 7 and eight hours after itaconate supplementation, is illustrated in the dose response curve (Figure  
17  
18 8 3B). It indicates that gene expression can be tuned in the range of approximately 0.07 to 0.7 mM for  
19  
20 9 a linear fluorescence output. The minimum concentration of exogenously added itaconate required  
21  
22 10 for activation of the system is approximately 0.016 mM. The dose response curve indicates a  
23  
24 11 saturation of the *YpItcR/P<sub>ccI</sub>* inducible system for itaconate levels above 2.5 mM. However, in order  
25  
26 12 for this system to be applied as biosensor for concentrations of more than 2.5 mM, its elements  
27  
28 13 require modification. This is commonly accomplished by promoter or protein engineering, both  
29  
30 14 strategies aiming to alter the binding affinity of the TR for either the operator sequence or the ligand  
31  
32 15 itself.<sup>39-41</sup> Notably, the concentration of exogenously added itaconate required to induce the system  
33  
34 16 in *E. coli* MG1655 is lower in LB medium than in M9 minimal medium. Four hours after addition of  
35  
36 17 0.016 mM itaconate, reporter gene expression is induced 7.7-fold in LB medium compared to a  
37  
38 18 culture without itaconate (Figure S3). This is in contrast to a 1.4-fold induction in M9 minimal  
39  
40 19 medium. The dose response curve indicates that the itaconate concentration, required for a linear  
41  
42 20 fluorescence output in LB medium, ranges between approximately 0.016-0.16 mM (Figure S3).

43  
44  
45 21 Despite a 5-fold reduced induction threshold for itaconate, the linear output range of the *YpItcR/P<sub>ccI</sub>*  
46  
47 22 inducible system spans one order of magnitude, similar to what is observed in M9 minimal medium.  
48  
49 23 This suggests that different growth conditions can contribute to the variation of both, lower and  
50  
51 24 upper induction thresholds, whereas the magnitude of system response is likely to remain constant.

52  
53  
54 25 In addition, the analysis of extracellular and intracellular itaconate by using high-  
55  
56 26 performance liquid chromatography (HPLC) coupled with ultraviolet (UV) spectroscopy shows no

1 significant change in the itaconate concentration during 12-hour period in the actively growing *E. coli*  
 2 culture (Table 2). This demonstrates that itaconate is not metabolized and therefore is a primary  
 3 inducing molecule. Moreover, the analysis confirms that itaconate is taken up by or diffuses into the  
 4 *E. coli* cell and reaches a relatively high concentration of at least 1.3 mM after 6 hours. It should be  
 5 noted that the actual intracellular molar concentration could be even higher, since our  
 6 approximation uses assumption that the intracellular cell volume is equal to the total cell volume  
 7 including the space occupied by cell membranes, lipids, etc. Interestingly, the intracellular itaconate  
 8 concentration becomes reduced when *E. coli* cells reach the stationary phase (12-hour time point,  
 9 Table 2), however the total itaconate concentration in the culture remains unchanged.

10  
 11 **Table 2.** Extracellularly added and intracellularly produced itaconate distribution between  
 12 supernatant and cells in *E. coli* culture grown in LB medium.

Itaconate extracellularly added					
Time (h)	Molar concentration (mM) <sup>a</sup>		Concentration in cell culture (mg/l)		
	Extracellular	Intracellular	Resulting from supernatant	Resulting from cells	Total
0	2.5 <sup>b</sup>	nd <sup>c</sup>	325.253	nd	325.253
	2.454 ±	1.309 ±			319.927 ±
6	0.050	0.132	319.242 ± 6.437	0.685 ± 0.067	6.437
	2.462 ±	0.551 ±			320.654 ±
12	0.059	0.058	320.243 ± 7.715	0.411 ± 0.074	7.715
Itaconate intracellularly produced					
Time (h)	Molar concentration (mM)		Normalized concentration in cell culture (mg/l/OD)		
	Extracellular	Intracellular	Resulting from supernatant (% of total)	Resulting from cells (% of total)	Total
0	nd	nd	nd	nd	nd
	0.071 ±	0.145 ±	2.149 ± 0.638		
18	0.021	0.008	(98.67)	0.029 ± 0.003 (1.33)	2.178
	0.242 ±	0.241 ±	7.010 ± 2.506		
36	0.117	0.181	(99.38)	0.044 ± 0.028 (0.62)	7.054

13 <sup>a</sup>Arithmetic mean ± standard deviation is derived using data of three biological replicates.

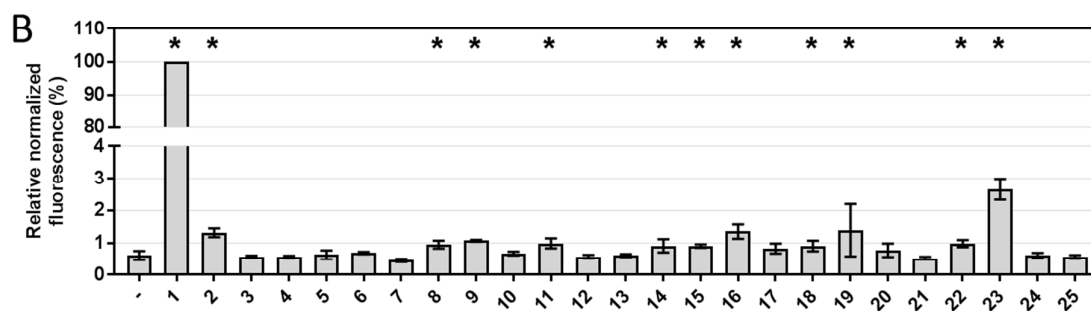
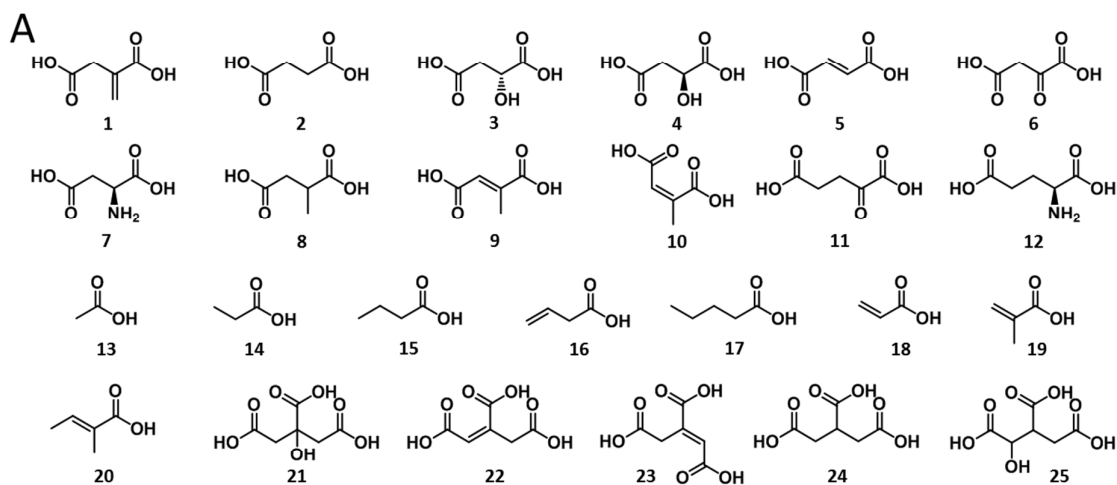
14 <sup>b</sup>Itaconate concentration added to cell culture at 0-hour time point.

15 <sup>c</sup>Not detected (nd).

1

2 **Sensor specificity**

3 The *YpltcR/P<sub>cdl</sub>* inducible system was analyzed for cross-induction by metabolites that may activate  
 4 reporter gene expression in the absence of the primary inducing molecule itaconate. These can be  
 5 exogenously added compounds or intermediates naturally involved in cellular metabolism.  
 6 Compounds that were investigated for cross-induction mainly include citric acid cycle intermediates  
 7 and structurally similar variants thereof (Figure 4A). Evaluation of these molecules may shed light on  
 8 structural features required for TR-binding and TR affinity towards itaconate. Furthermore,  
 9 screening potential candidate compounds might expand the list of metabolites to be detected by TR-  
 10 based controllable systems and offer the possibility to be utilized as analogue inducers to control  
 11 gene expression.



12

1  
2  
3 **Figure 4.** Inducer-dependent orthogonality of the *YpltcR/P<sub>ccI</sub>* inducible system. (A) Compounds that  
4 were investigated for cross-induction with the *YpltcR/P<sub>ccI</sub>* inducible system: itaconic acid (1), succinic  
5 acid (2), D-malic acid (3), L-malic acid (4), fumaric acid (5), oxaloacetic acid (6), L-aspartic acid (7),  
6 methylsuccinic acid (8), mesaconic acid (9), citraconic acid (10),  $\alpha$ -ketoglutaric acid (11), L-glutamic  
7 acid (12), acetic acid (13), propionic acid (14), butyric acid (15), 3-butenoic acid (16), valeric acid (17),  
8 acrylic acid (18), methacrylic acid (19), tiglic acid (20), citric acid (21), *cis*-aconitic acid (22), *trans*-  
9 aconitic acid (23), tricarballic acid (24), isocitric acid (25). (B) Normalized fluorescence (in %) of *E.*  
10 *coli* MG1655 harboring the *YpltcR/P<sub>ccI</sub>* inducible system twelve hours after addition of different  
11 compounds at a final concentration of 5 mM, relative to the fluorescence output obtained by adding  
12 5 mM itaconate. (-), uninduced sample. Error bars represent standard deviations of three biological  
13 replicates. Asterisks indicate statistically significant induction values for  $p < 0.01$  (unpaired *t* test).

14  
15  
16  
17  
18  
19  
20  
21  
22  
23  
24  
25  
26  
27  
28  
29  
30  
31  
32  
33  
34  
35  
36  
37  
38  
39  
40  
41  
42  
43  
44  
45  
46  
47  
48  
49  
50  
51  
52  
53  
54  
55  
56  
57  
58  
59  
60

The fluorescence output from cultures of *E. coli* MG1655 harboring the *YpltcR/P<sub>ccI</sub>* inducible system, and cultivated in M9 minimal medium, was monitored over time after individual addition of each compound at a final concentration of 5 or 10 mM. Normalized fluorescence levels (in %), relative to the output obtained by adding 5 mM itaconate, were determined twelve hours after compound supplementation. In addition to the primary inducer itaconate and under the assumption that all tested metabolites are able to enter the cell, the compounds succinate (2), methylsuccinate (8), mesaconate (9),  $\alpha$ -ketoglutarate (11), propionate (14), butyrate (15), 3-butenoate (16), acrylate (18), methacrylate (19), *cis*-aconitate (22), and *trans*-aconitate (23) induce reporter gene expression at a final concentration of 5 mM with high statistical significance ( $p < 0.01$ ) (Figure 4B). Of these eleven compounds, succinate, mesaconate, propionate, butyrate, 3-butenoate, *cis*-aconitate and *trans*-aconitate demonstrated a significant increase in RPF expression at a final concentration of 10 mM (Figure S4). Increased activation of reporter gene expression suggests that these inducers may exhibit a weak binding to TR inducing the system to some extent. The highest level of cross-induction is mediated by *trans*-aconitate. At a concentration of 10 mM, it reached 9.9% of the

1 absolute normalized fluorescence that was achieved by using 5 mM itaconate. Since *E. coli* has not  
2 been reported to encode a *trans*-aconitate decarboxylase, converting *trans*-aconitate into itaconate,  
3 induction of reporter gene expression from *YpP<sub>cci</sub>* is more likely to be caused by ItcR promiscuity  
4 rather than by decarboxylation of *trans*-aconitate forming itaconate.

5 *Cis*- and *trans*-aconitate showed more than a two-fold change in induction level when  
6 inducer concentration was two-fold increased from 5 to 10 mM suggesting that these compounds  
7 may activate the system at higher concentrations. To obtain a more accurate resolution of their dose  
8 responses, the *YpItcR/P<sub>cci</sub>* inducible system was subjected to a range of concentrations of *cis*-, and  
9 *trans*-aconitate. Since mesaconate has been previously shown to act as CoA acceptor by *Yplct*, with  
10 second lowest  $K_m$  after itaconate,<sup>32</sup> this compound was also included in the dose response  
11 experiment.

12 A saturation in fluorescence output when using mesaconate, *cis*-, or *trans*-aconitate as  
13 inducer was not possible to obtain. All three inducers demonstrated some degree of toxicity  
14 inhibiting cell growth at higher concentrations. However, based on a phenomenological model for  
15 metabolite biosensors,<sup>41</sup> it can be postulated that the maximal dynamic range of an inducible  
16 system, which is the maximal level of expression relative to basal promoter activity, is not affected  
17 by metabolite-TR affinity. Therefore, the maximal dynamic range calculated for itaconate as inducer  
18 was employed to fit the dynamic range data for mesaconate, *cis*-, and *trans*-aconitate using a Hill  
19 function (Figure S5). The resulting  $K_i$ , the extracellularly added-inducer concentration which  
20 mediates half-maximal RFP expression, is different for each of these compounds. They reveal that  
21 mesaconate, *cis*-, and *trans*-aconitate  $K_i$  values are higher (45.2 mM, 31.1 mM, and 13.2 mM,  
22 respectively) and therefore activate the *YpItcR/P<sub>cci</sub>* inducible system at much higher extracellular  
23 concentrations than itaconate ( $K_i = 0.43$  mM). The structural characteristics may contribute to the  
24 ability of metabolites to interact with ItcR and act as inducers. Indeed, mesaconate, *cis*-, and *trans*-  
25 aconitate have structural similarities to itaconate, with last two harboring the complete itaconate  
26 element. However, the observation that all three compounds have a much higher  $K_i$  than itaconate

1 suggests, that for maximal activation of the *YpItcR/P<sub>ccI</sub>* inducible system, the unmodified itaconate  
2 structure is indispensable. It also suggests that the binding affinity of the TR to a specific ligand may  
3 play an important role. Consequently, protein engineering of ItcR may be used to change the binding  
4 affinity for itaconate. On the other hand, it cannot be excluded that the change in inducer dynamic  
5 range is affected by the differential uptake of these compounds by the *E. coli* cell.

6 It should be noted that acetate, propionate, butyrate, methylsuccinate, and mesaconate  
7 have previously been demonstrated to act as CoA acceptors by *YpIct*, albeit at a much higher  $K_m$  than  
8 itaconate,<sup>32</sup> suggesting that these compounds might be secondary inducers of the *YpItcR/P<sub>ccI</sub>*  
9 inducible system. Interestingly, their level of induction correlates with their ability to act as CoA  
10 acceptors, with acetate, propionate and butyrate having a higher, and mesaconate having a lower  
11  $K_m$ .<sup>32</sup> Furthermore, the catalytic efficiency ( $k_{cat}/K_m$ ) of *YpIct* with itaconate, mesaconate,  
12 methylsuccinate, butyrate, propionate, and acetate,<sup>32</sup> shows a high level of direct correlation with  
13 level of induction by these compounds. This suggests there might be structural evolutionary link  
14 between enzyme (*YpIct*) and transcriptional regulator (ItcR), where both proteins have co-evolved  
15 enabling a hierarchical ranking of metabolites as enzyme substrates and TR activators in the  
16 following order: itaconate > mesaconate > methylsuccinate > butyrate > propionate > acetate. The  
17 direct correlation between catalytic efficiency and level of induction potentially ensures that the  
18 hierarchy is supported at the gene expression and enzyme activity levels by securing the highest  
19 level of *YpIct* synthesis and highest catalytic efficiency when itaconate is present in the environment.  
20 Overall, the *YpItcR/P<sub>ccI</sub>* inducible system demonstrates a high specificity towards itaconate and may  
21 therefore be used in combination with other inducible systems to orthogonally control gene  
22 expression in biosynthetic pathways composed of multiple genes.

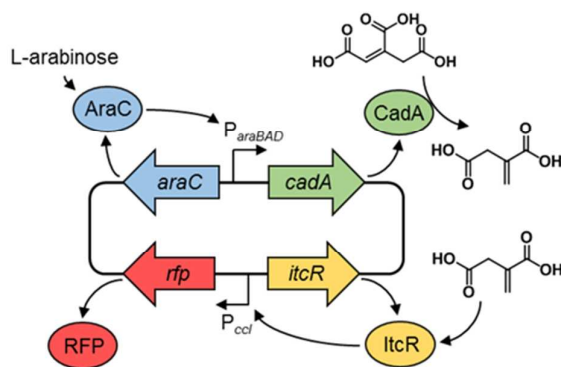
### 23 Biosensor-assisted optimization of itaconic acid production

24 Itaconic acid can be synthesized by decarboxylation of the citric acid cycle intermediate *cis*-aconitic  
25 acid. This reaction is catalyzed by *cis*-aconitate decarboxylase (CadA). The *A. terreus cadA* gene has

1  
2  
3 1 previously been expressed in *E. coli* for the biosynthesis of itaconate by using either a constitutive  
4  
5 2 promoter, or an inducible T7 polymerase-based expression system.<sup>13, 20, 42</sup> Overexpression of *cadA*  
6  
7 3 was reported to impair cellular growth,<sup>42</sup> suggesting that fine-tuning of CadA levels is essential to  
8  
9 4 ensure optimal metabolic flux. Even though the pathway for itaconate biosynthesis in *E. coli* solely  
10  
11 5 requires the introduction of one additional gene, balancing its expression and quantitatively  
12  
13 6 evaluating its impact on itaconate production can be laborious when using standard analytical  
14  
15 7 techniques. We decided to apply the *YpItcR/P<sub>ccI</sub>* inducible system to monitor itaconate production by  
16  
17 8 fluorescence output in response to different levels of CadA.

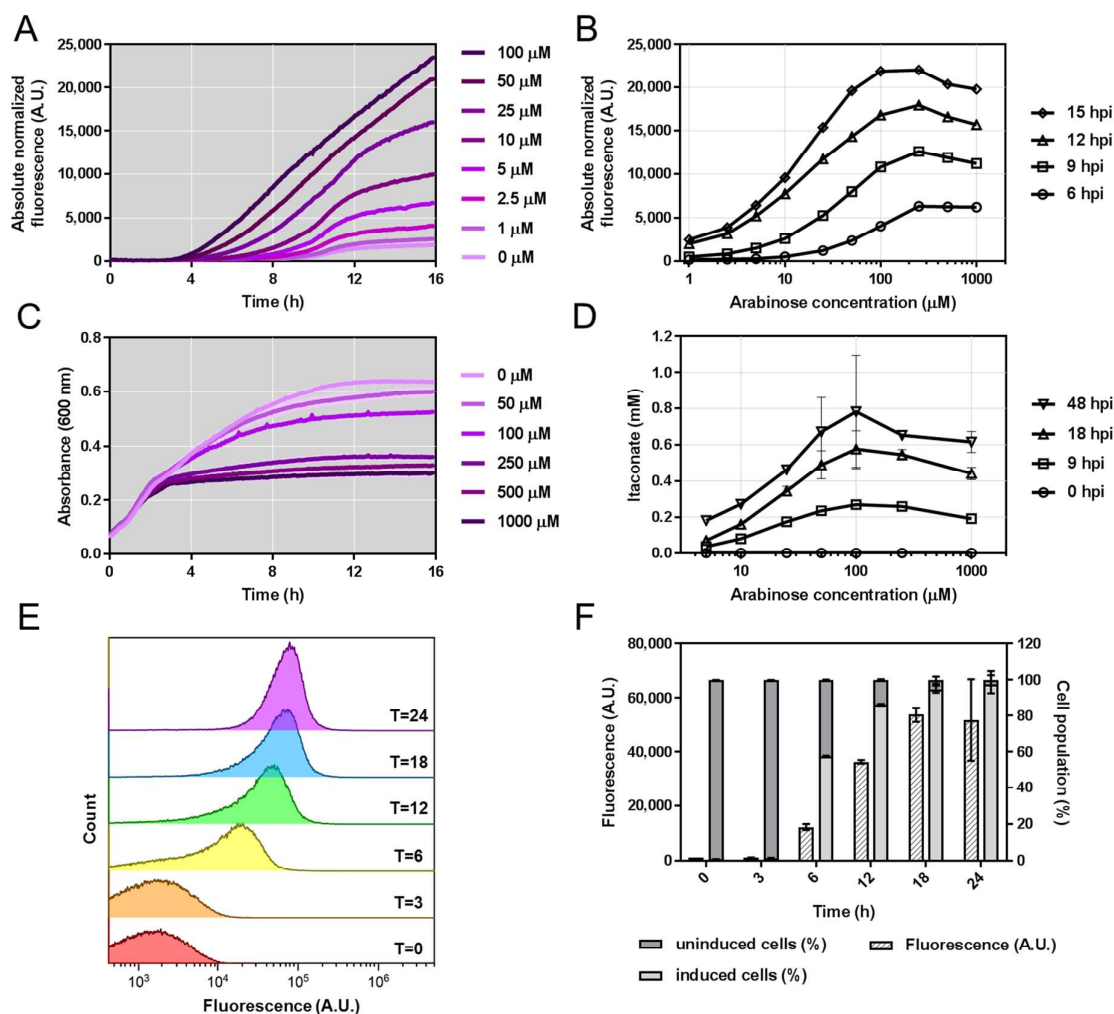
19  
20 9 A single plasmid (pEH165) was constructed that contains two modules: one for itaconate  
21  
22 10 production and one for itaconate sensing (Figure 5). The *A. terreus cadA* (ATEG\_09971) coding  
23  
24 11 sequence was cloned downstream of the arabinose-inducible system and a T7 mRNA stem-loop  
25  
26 12 structure sequence, which was incorporated to enhance *cadA* mRNA stability.<sup>43</sup> The itaconate  
27  
28 13 sensing module contains the *YpItcR/P<sub>ccI</sub>* inducible system in combination with the *rfp* reporter gene.  
29  
30 14 Addition of L-arabinose to cells harboring this plasmid was expected to initiate *cadA* expression,  
31  
32 15 resulting in biosynthesis of itaconate and subsequent activation of reporter gene expression. *E. coli*  
33  
34 16 TOP10 was transformed with plasmid pEH165 and cells in early exponential growth phase were  
35  
36 17 transferred to a 96-well microtiter plate. Subsequently, growth and fluorescence were monitored  
37  
38 18 over time after supplementation with different concentrations of L-arabinose ranging from 1 to 1000  
39  
40 19  $\mu\text{M}$ . As it can be seen in the fluorescence curve of induction kinetics, higher concentrations of L-  
41  
42 20 arabinose mediate a faster fluorescence output (Figure 6A). Reporter gene expression above  
43  
44 21 background levels can be observed 150 minutes after addition of 100  $\mu\text{M}$  L-arabinose, whereas 10  
45  
46 22  $\mu\text{M}$  require about one hour more. The dose response curve indicates that maximum absolute  
47  
48 23 normalized fluorescence is achieved by supplementation with 250  $\mu\text{M}$  L-arabinose (Figure 6B). This  
49  
50 24 suggests that expression of *cadA* can be fine-tuned when using inducer concentrations in the range  
51  
52 25 between 1 and 100  $\mu\text{M}$ . L-arabinose concentrations of 0.5 and 1 mM, however, appear to negatively  
53  
54 26 impact reporter gene expression, indicating a drop in itaconate levels. The negative effect of high  
55  
56  
57  
58  
59  
60

1 inducer levels becomes even more evident from the absorbance data, showing that L-arabinose  
 2 concentrations of 250  $\mu$ M and more reduce cell density considerably (Figure 6C). Most likely, this  
 3 behaviour results from an increased metabolic burden caused by overproduction of CadA, as  
 4 mentioned earlier.<sup>42</sup>



5  
 6 **Figure 5.** Schematic illustration of the plasmid containing both an itaconate production and sensing  
 7 module. Exogenous addition of L-arabinose initiates synthesis of the *cis*-aconitate decarboxylase  
 8 CadA which converts *cis*-aconitate into itaconate. RFP reporter gene expression is subsequently  
 9 mediated by ItcR in the presence of itaconate.

10



1

2 **Figure 6.** Biosensor-assisted optimization of itaconate production. (A) Absolute normalized  
 3 fluorescence of *E. coli* TOP10 harboring pEH165, grown in microtiter plates, in response to 1-100  $\mu\text{M}$   
 4 of L-arabinose supplemented at time zero. The means of three biological replicates are presented.  
 5 Error bars are too small to be visible. (B) Dose response curve of *E. coli* TOP10 harboring pEH165,  
 6 grown in microtiter plates, 6, 9, 12, and 15 hours post induction (hpi) with 1-1000  $\mu\text{M}$  of L-arabinose.  
 7 The means of three biological replicates are presented. Error bars are too small to be visible. (C)  
 8 Absorbance at 600 nm of *E. coli* TOP10 harboring pEH165, grown in microtiter plates, in response to  
 9 50-1000  $\mu\text{M}$  of L-arabinose supplemented at time zero. The means of three biological replicates are  
 10 presented. The standard deviation for 50  $\mu\text{M}$  of inducer is illustrated as lighter colour ribbon  
 11 displayed lengthwise the growth curve. The error bars for the other inducer concentrations are too

1  
2  
3 1 small to be visible. (D) Itaconate titers of *E. coli* TOP10 harboring pEH165, grown in small-volume  
4  
5 2 cultures, 0, 9, 18, and 48 hours post induction with 5, 10, 25, 50, 100, 250, and 1000  $\mu\text{M}$  of L-  
6  
7 3 arabinose. Error bars represent standard deviations of three biological replicates. (E) Flow  
8  
9 4 cytometric analysis of *E. coli* TOP 10 harboring pEH165, grown in small-volume cultures, in response  
10  
11 5 to 100  $\mu\text{M}$  of L-arabinose. Samples were taken 0, 3, 6, 12, 18 and 24 hours after inducer addition.  
12  
13 6 For the time points T=6, T=12, T=18 and T=24, fluorescence from more than 99% of cells are  
14  
15 7 displayed in the histogram, whereas for time points T=0 and T=3, less than 25% of cells are below  
16  
17 8 429 A. U. fluorescence threshold in the histogram. (F) Fluorescence intensity (median) and  
18  
19 9 percentage of uninduced and induced cells corresponding to the data presented in panel E. Error  
20  
21 10 bars represent standard deviations of three biological replicates.  
22  
23  
24  
25  
26

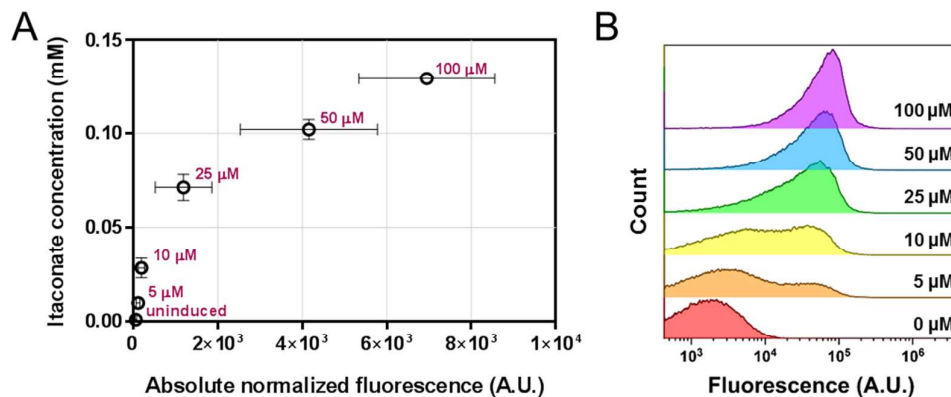
27 12 To quantitatively validate the data which was generated from cultures grown in microtiter  
28  
29 13 plates, the experiment was repeated in small culture volumes. *E. coli* TOP10 pEH165 was grown in  
30  
31 14 50-mL culture tubes and expression of *cadA* was initiated by supplementation with different  
32  
33 15 concentrations of L-arabinose. To determine itaconate titers, samples were subjected to the analysis  
34  
35 16 using HPLC-UV. The highest itaconate concentration was achieved in cultures containing 100  $\mu\text{M}$  L-  
36  
37 17 arabinose, resulting in  $0.78 \pm 0.31$  mM itaconate 48 hours after inducer addition (Figure 6D). This  
38  
39 18 represents a 4.3-fold improvement over cultures containing only 5  $\mu\text{M}$  L-arabinose. It should be  
40  
41 19 noted that these and data in Table 2 demonstrate that the intracellularly synthesised itaconate was  
42  
43 20 actively excreted or diffused into the media.  
44

45 21 Addition of an excessive amount of 1 mM inducer also decreased itaconate levels by 1.3-  
46  
47 22 fold. Therefore, the quantitative data obtained from the small-volume cultures match well with the  
48  
49 23 fluorescence output measured in the microtiter plate (compare Figure 6B and 6D). Particularly when  
50  
51 24 itaconate titers are OD-normalized, 250  $\mu\text{M}$  L-arabinose results in the highest OD-normalized  
52  
53 25 itaconate titer (Figure S6). This experiment illustrates that *cadA* expression needs to be carefully  
54  
55 26 fine-tuned to guarantee both optimal metabolic flux and viability of cells.  
56  
57  
58  
59  
60

1  
2  
3 1 Moreover, using 100  $\mu$ M of L-arabinose yields itaconate concentrations of 0.24, 0.56 and  
4  
5 2 0.78 mM after 9, 18 and 48 hours post induction, respectively (Figure 6D). These itaconate  
6  
7 3 concentrations fall within the linear range of dose response (Figure 3B) and result in a fluorescence  
8  
9 4 output with a unimodal distribution suggesting that almost all cells in the population were activated  
10  
11 5 (Figure 6E and 6F). As demonstrated here, the itaconate biosensor can be employed to facilitate a  
12  
13 6 fluorescence-based high-throughput screen to evaluate various conditions for their impact on  
14  
15 7 itaconate biosynthesis.  
16  
17  
18

### 8 Correlation between biosensor output and itaconate concentration

9 In addition to HPLC-UV analysis, the samples from the small-volume cultures of *E. coli* TOP10 pEH165  
10  
11 10 were analyzed for fluorescence output. The obtained data were used to evaluate whether  
12  
13 11 quantitatively determined itaconate titers correlate with reporter gene expression from the  
14  
15 12 biosensor. The five tested inducer concentrations that did not impair bacterial growth produced a  
16  
17 13 59-fold range in fluorescence after six hours (Figure 7A). The addition of 25, 50 and 100  $\mu$ M L-  
18  
19 14 arabinose resulted in itaconate titers that were sufficiently high to be detected by the biosensor.  
20  
21 15 Notably, in the linear response range of the  $Y_{pItcR}/P_{ccI}$  inducible system, the fluorescence output  
22  
23 16 shows a high level of correlation with HPLC-UV-measured extracellular itaconate titers (Figure 7A)  
24  
25 17 and unimodal fluorescence distribution in the cell population (Figure 7B). L-arabinose concentrations  
26  
27 18 of 5 and 10  $\mu$ M result in a bimodal fluorescence response, suggesting an all-or-none induction in  
28  
29 19 which intermediate inducer concentrations give rise to subpopulations. However, when different  
30  
31 20 levels of itaconate are synthesized in the range between 0.1 and 0.78 mM, which corresponds to the  
32  
33 21 linear response range, the fluorescence output becomes unimodal (Figures 6D, 6E and 7A). This  
34  
35 22 confirms that for itaconate levels in the linear range, the  $Y_{pItcR}/P_{ccI}$  inducible system mediates a  
36  
37 23 homogenous induction of cells, exemplifying its potential to fine-tune gene expression across cell  
38  
39 24 populations and to be utilized as a quantitatively reliable biosensor.  
40  
41  
42  
43  
44  
45  
46  
47  
48  
49  
50  
51  
52  
53  
54  
55  
56  
57  
58  
59  
60



1

2 **Figure 7.** Correlation between biosensor output and itaconate concentration. (A) Absolute  
 3 normalized fluorescence values of *E. coli* TOP10 pEH165 are correlated with their corresponding  
 4 itaconate concentration in the culture supernatant. Samples were taken six hours after inducer  
 5 addition. The different concentrations of exogenously added L-arabinose, ranging from 5 to 100  $\mu\text{M}$ ,  
 6 are highlighted. Error bars represent standard deviations of three biological replicates. (B) Flow  
 7 cytometric analysis of samples from panel A. For L-arabinose (inducer) concentrations of 25, 50, and  
 8 100  $\mu\text{M}$ , fluorescence from more than 99% of cells are displayed in the histogram, whereas for  
 9 concentrations of 10, 5 and 0  $\mu\text{M}$ , less than 2, 10 and 25% of cells, respectively, are below 429 A. U.  
 10 fluorescence threshold in the histogram.

11

## 1 Methods

### 2 Base strains and media

3 *E. coli* TOP10 (Invitrogen) was used for cloning, plasmid propagation, and biosynthesis of itaconate.  
4 RFP fluorescence assays for biosensor characterization were performed in wild type *E. coli* MG1655  
5 (DSMZ 18039) and *C. necator* H16 (ATCC 17699). Bacterial strains were propagated in LB medium.  
6 For reporter gene assays, *E. coli* MG1655 was cultivated in M9 minimal medium<sup>44</sup> supplemented  
7 with 1 µg/L thiamine, 20 µg/mL uracil<sup>45</sup> and 0.4% (w/v) glucose, unless otherwise indicated. *C.*  
8 *necator* reporter gene assays were performed in minimal medium<sup>46</sup> containing 0.4% (w/v) sodium  
9 gluconate. Antibiotics were added to the growth medium at the following concentrations: 25 µg/mL,  
10 or 50 µg/mL chloramphenicol for *E. coli*, or *C. necator*, respectively. *E. coli* TOP10 was grown at 30 or  
11 37°C. For comparison, both *E. coli* MG1655 and *C. necator* were cultivated at 30°C.

### 12 Cloning and transformation

13 Plasmid minipreps were carried out using the New England BioLabs (NEB) Monarch® Plasmid  
14 Miniprep Kit. Microbial genomic DNA was extracted employing the GenElute™ Bacterial Genomic  
15 DNA Kit (Sigma). For cloning, DNA was amplified by PCR using Phusion High-Fidelity DNA polymerase  
16 from NEB in 50 µL reactions under recommended conditions. Restriction enzymes and NEBuilder Hifi  
17 DNA assembly master mix were purchased from NEB and reactions were set up according to the  
18 manufacturer's protocol. The NEB Monarch® DNA Gel Extraction Kit was used to extract gel purified  
19 linearized DNA which was subsequently used for cloning.

20 Chemical competent *E. coli* were prepared and transformed by heat shock as previously  
21 described.<sup>44</sup> Electrocompetent *C. necator* were prepared and transformed as reported by Ausubel et  
22 al.<sup>47</sup>

## 1 Plasmid construction

2 Oligonucleotide primers were synthesized by Sigma-Aldrich (Table S1). Plasmids were constructed by  
3 employing either the NEBuilder Hifi DNA assembly method according to the manufacturer's protocol  
4 or by restriction enzyme-based cloning procedures.<sup>44</sup> Constructs were verified by DNA sequencing  
5 (Source BioScience, Nottingham, UK). The nucleotide sequences of pEH086 and pEH177 have been  
6 deposited in the public version of the ACS registry (<https://acs-registry.jbei.org>) under the accession  
7 number ACS\_000716 and ACS\_000717, respectively.

8 The itaconate-inducible systems *YpItcR/P<sub>ccI</sub>* and *PaItcR/P<sub>ich</sub>* were amplified with  
9 oligonucleotide primers EH191\_f and EH190\_r, EH312\_f and EH311\_r, respectively, from *Y.*  
10 *pseudotuberculosis* YPIII (*Yp*) and *P. aeruginosa* PAO1 (*Pa*) genomic DNA and cloned into pEH006 by  
11 AatII and NdeI restriction sites (resulting in plasmids pEH086 and pEH177). The itaconate-inducible  
12 promoters *YpP<sub>ccI</sub>* and *PaP<sub>ich</sub>* were amplified with oligonucleotide primers EH191\_f and EH302\_r,  
13 EH312\_f and EH313\_r, respectively, from *Y. pseudotuberculosis* YPIII and *P. aeruginosa* PAO1  
14 genomic DNA and cloned into pEH006 by AatII and NdeI restriction sites (resulting in plasmids  
15 pEH172 and pEH178).

16 Vector pEH164 contains both the itaconate-reporter system composed of *YpItcR-P<sub>ccI</sub>-rfp* and  
17 the L-arabinose-inducible system including restriction sites for subsequent integration of the *cis*-  
18 aconitate decarboxylase *cadA* gene (ATEG\_09971) downstream of *P<sub>araBAD</sub>*. It was constructed by  
19 employing the NEBuilder Hifi DNA assembly method. Oligonucleotide primers EH011\_f and EH075\_r,  
20 EH015\_f and EH012\_r, EH078\_f and EH190\_r, EH083\_f and EH079\_r were used to amplify the  
21 replication origin and the chloramphenicol resistance gene, *YpItcR-P<sub>ccI</sub>-rfp*, and the L-arabinose-  
22 inducible system from pBBR1MCS-2-PphaC-eyfp-c1, pEH086, and pEH006, respectively.<sup>36, 37</sup>

23 Vector pEH165 contains both the itaconate-production system *AraC-P<sub>araBAD</sub>-cadA* and the  
24 itaconate-reporter system *YpItcR-P<sub>ccI</sub>-rfp*. Oligonucleotide primers EH294\_f and EH293\_r, EH296\_f  
25 and EH295\_r were used to amplify exon 1 and exon 2 of ATEG\_09971 from *A. terreus* NIH2642

1 genomic DNA. The PCR products were combined with BglII/SbfI digested pEH164 and constructed by  
2 employing the NEBuilder HiFi DNA assembly method.

### 3 RFP fluorescence assay

4 RFP fluorescence was measured with an Infinite® M1000 PRO (Tecan) micro plate reader using 585  
5 nm as excitation and 620 nm as emission wavelength. The gain factor was set manually to 100%.  
6 Absorbance was determined at 600 nm to normalize fluorescence by optical density. Fluorescence  
7 and absorbance readings at a single time point, and over time, were performed as described  
8 previously.<sup>36</sup> The absolute normalized fluorescence was calculated by dividing the absolute  
9 fluorescence values by their corresponding absorbance values. Prior normalization, both values were  
10 corrected by the auto-fluorescence and -absorbance of the culture medium.

### 11 Production of itaconate and HPLC-UV analysis

12 Real-time biosynthesis of itaconate was monitored quantitatively by high-performance liquid  
13 chromatography (HPLC) in combination with ultraviolet (UV) absorbance at 210 nm and by  
14 fluorescence output in *E. coli* T10 harboring pEH165. Single colonies of freshly transformed cells  
15 were used to inoculate five mL LB medium. The preculture was incubated for 18 hours at 37°C and  
16 200 rpm. Subsequently, it was diluted 1:100 in six mL fresh LB medium. The main cultures were  
17 grown in 50-mL Falcon tubes at 30°C and 225 rpm. At an OD<sub>600</sub> of 0.5, 50 µL of L-arabinose stock  
18 solutions were added to achieve the final concentrations of 5, 10, 25, 50, 100, 250 and 1000 µM.  
19 One sample per biological replicate remained uninduced. Samples of 0.5 mL were taken  
20 immediately, 6, 9, 12, 18, 24, and 48 hours after inducer supplementation. They were directly used  
21 for evaluation by flow cytometry, OD<sub>600</sub> and fluorescence measurement. The remaining sample was  
22 centrifuged for 5 min at 16,000 × *g*, and the cell-free supernatant was subjected to HPLC-UV analysis  
23 as reported previously.<sup>36</sup>

## 1 Metabolite extraction

2 To determine intracellular itaconate concentrations when added extracellularly or synthesized  
3 intracellularly, cultures of *E. coli* TOP10 harboring pEH164 or pEH165 were grown overnight to  
4 saturation and diluted 1:100 in 200 mL LB medium. The main cultures were grown in 1-L shake flasks  
5 at 30°C and 225 rpm. At an OD<sub>600</sub> of 0.5, inducers were added at final concentrations of 2.5 mM  
6 itaconate or 100 μM L-arabinose to cultures of *E. coli* TOP10 harboring pEH164 or pEH165,  
7 respectively. Samples of cells containing pEH164 were taken 0, 6 and 12 hours after addition of  
8 itaconate. Samples of cells containing pEH165 were taken 0, 18 and 36 hours after addition of L-  
9 arabinose. Each time, the culture volume corresponding to an OD<sub>600</sub> of 50 was centrifuged for 10 min  
10 at 16,000 × *g*. The supernatant was removed and stored at -80°C for HPLC analysis. Subsequently,  
11 the cell pellet was washed once in 1 mL of phosphate buffered saline (PBS), transferred to a  
12 microcentrifuge tube and centrifuged as before. The supernatant was completely removed, the  
13 pellet was weighed using fine balance and frozen overnight at -80°C.

14 The extraction of intracellular metabolites including itaconate was performed as described  
15 previously<sup>48</sup> with modifications as described below. Briefly, 250 μL of -40°C cold methanol-water  
16 solution (60% v/v) was added to the wet cell pellet with the volume of 50-70 μL. Subsequently, the  
17 sample was mixed vigorously using vortex until completely resuspended. The cell suspension was  
18 frozen at -80°C for 30 min, thawed on ice and vortexed vigorously for 1 min. This step was repeated  
19 three times before the sample was centrifuged at -10°C and 26,000 × *g* for 20 min. The supernatant  
20 was collected and kept at -80°C. To the pellet, another 250 μL of -40°C cold methanol-water solution  
21 (60% v/v) was added. The cells were resuspended completely using vortex, three freeze-thaw cycles  
22 performed as above and centrifuged as before. The supernatant was pooled with the first one and  
23 stored at at -80°C until subjected to HPLC analysis.

## 1 Calculation of intracellular itaconate concentration in cell culture

2 The total cell volume ( $V_{\text{pellet}}$ ) in the sample was calculated by dividing the weight of wet cell pellet by  
3 the cell density of 1.105 g/mL.<sup>49</sup> Together with the volume of extraction solvent added to the  
4 sample,  $V_{\text{pellet}}$  was used to calculate the dilution factor required to determine the intracellular molar  
5 concentration of itaconate. Subsequently, the intracellular itaconate concentration in the cell culture  
6 ( $C_{\text{intracellular/CC}}$ ) was calculated using equation:

$$C_{\text{intracellular/CC}} = \frac{FW_{\text{itaconic acid}} \cdot C_{\text{molar}} \cdot V_{\text{pellet}}}{V_{\text{culture}}}$$

7 The remaining parameters correspond to the formula weight of itaconic acid ( $FW_{\text{itaconic acid}}$ ), the  
8 intracellular molar concentration of itaconate determined by HPLC-UV ( $C_{\text{molar}}$ ) and the culture  
9 volume sampled ( $V_{\text{culture}}$ ).

## 10 Flow cytometry

11 Cells were analyzed for induction homogeneity by flow cytometry. The culture sample was  
12 centrifuged for 4 min at 5,000  $\times g$ . Subsequently, the cell pellet was resuspended in cold and sterile  
13 filtered PBS to an OD<sub>600</sub> of 0.01 and kept on ice until analyzed using an Astrios EQ flow cytometer  
14 (Beckman Coulter) equipped with a 561 nm laser and a 614/20 nm emission band-pass filter. The  
15 voltage of photomultiplier tube (PMT) was set to 400 volts. The area and height gain was adjusted to  
16 1.0. For each sample, at least 100,000 events were collected. The data was analyzed using software  
17 Kaluza 1.5 (Beckman Coulter). To determine the percentage of induced cells, gating was performed  
18 on the uninduced sample to include 99% of cells. The same gate was subsequently applied to each  
19 induced sample.

## 20 Calculation of half-maximal RFP expression

21 Due to toxicity at higher levels, the concentrations of mesaconate, *cis*-, and *trans*-aconitate, which  
22 mediate half-maximal RFP expression ( $K_i$ ), were predicted using a phenomenological model as  
23 described previously.<sup>41</sup> The model describes the change in dynamic range of an inducible system as a

1  
2  
3  
4  
5  
6  
7  
8  
9  
10  
11  
12  
13  
14  
15  
16  
17  
18  
19  
20  
21  
22  
23  
24  
25  
26  
27  
28  
29  
30  
31  
32  
33  
34  
35  
36  
37  
38  
39  
40  
41  
42  
43  
44  
45  
46  
47  
48  
49  
50  
51  
52  
53  
54  
55  
56  
57  
58  
59  
60

1 function of inducer concentration. It assumes that: 1) the maximum dynamic range of a biosensor  
2 ( $\mu_{\max}$ ) remains constant as long as the genetic context does not change, and 2)  $K_i$  is dependent on  
3 metabolite-TR affinity.

4 The dynamic range ( $\mu$ , also referred to as induction factor) for each concentration of  
5 itaconate was calculated using the absolute normalised fluorescence values from the time course  
6 experiment six hours after itaconate addition. After subtraction of the basal output, the resulting  
7 dynamic range was fit to the corresponding inducer concentration using the Hill function:

$$\mu(I) = \mu_{\max} \cdot \frac{I^h}{K_i^h + I^h}$$

8 The remaining parameters correspond to concentration of inducer ( $I$ ), and the Hill coefficient ( $h$ ).  
9 Subsequently, the itaconate  $\mu_{\max}$  was used as fixed parameter to calculate  $K_i$  for mesaconate, *cis*-,  
10 and *trans*-aconitate employing the same Hill function. The fitted data is illustrated in Figure S5.  
11 Calculations were performed using Prism GraphPad software version 7.03.

12

## 1 Associated content

### 2 Supporting information

3 Further experimental details for plasmid construction and additional figures described in the main  
4 text.

## 5 Author information

### 6 Corresponding author

7 E-mail: Naglis.Malys@nottingham.ac.uk

### 8 Author contribution

9 E.H. and N.M designed the study. E.H. performed the experiments. E.H., N.M. and N.P.M. analyzed  
10 the data and wrote the manuscript.

### 11 Conflict of interest

12 The authors declare that they have no competing interests.

## 13 Acknowledgements

14 This work was supported by the Biotechnology and Biological Sciences Research Council [grant  
15 number BB/L013940/1] (BBSRC); and the Engineering and Physical Sciences Research Council  
16 (EPSRC) under the same grant number. We thank University of Nottingham for providing SBRC-  
17 DTProg PhD studentship to E.H., Swathi Alagesan for preliminary work on itaconate production in *C.*  
18 *necator* H16, Matthew Abbott and David Onion for assistance with HPLC analysis and flow  
19 cytometry, Thomas Millat for discussion on data analysis, Amy Slater, Carolina Paiva, Matthias Brock  
20 and Elena Geib for gifting *Y. pseudotuberculosis*, *P. aeruginosa* and *A. terreus* genomic DNA and all  
21 members of SBRC who helped to carry out this research.

22

## 1 References

- 2 [1] Clomburg, J. M., Crumbley, A. M., and Gonzalez, R. (2017) Industrial  
3 biomanufacturing: The future of chemical production. *Science* 355 (6320),  
4 aag0804.
- 5 [2] Latif, H., Zeidan, A. A., Nielsen, A. T., and Zengler, K. (2014) Trash to treasure:  
6 production of biofuels and commodity chemicals via syngas fermenting  
7 microorganisms. *Curr. Opin. Biotechnol.* 27, 79-87.
- 8 [3] Keasling, J. D. (2010) Manufacturing molecules through metabolic engineering.  
9 *Science* 330 (6009), 1355-1358.
- 10 [4] Okabe, M., Lies, D., Kanamasa, S., and Park, E. Y. (2009) Biotechnological  
11 production of itaconic acid and its biosynthesis in *Aspergillus terreus*. *Appl.*  
12 *Microbiol. Biotechnol.* 84 (4), 597-606.
- 13 [5] Werpy, T., Petersen, G., Aden, A., Bozell, J., Holladay, J., White, J., Manheim, A.,  
14 Eliot, D., Lasure, L., and Jones, S. (2004) Top value added chemicals from  
15 biomass. Volume 1-Results of screening for potential candidates from sugars  
16 and synthesis gas, Department of Energy Washington DC.
- 17 [6] Choi, S., Song, C. W., Shin, J. H., and Lee, S. Y. (2015) Biorefineries for the  
18 production of top building block chemicals and their derivatives. *Metab. Eng.*  
19 28, 223-239.
- 20 [7] Bentley, R., and Thiessen, C. P. (1957) Biosynthesis of itaconic acid in *Aspergillus*  
21 *terreus*: I. Tracer studies with C<sup>14</sup>-labeled substrates. *J. Biol. Chem.* 226 (2),  
22 673-687.
- 23 [8] Haskins, R., Thorn, J., and Boothroyd, B. (1955) Biochemistry of the Ustilaginales:  
24 XI. Metabolic products of *Ustilago zaeae* in submerged culture. *Can. J.*  
25 *Microbiol.* 1 (9), 749-756.
- 26 [9] Tabuchi, T., Sugisawa, T., Ishidori, T., Nakahara, T., and Sugiyama, J. (1981)  
27 Itaconic acid fermentation by a yeast belonging to the genus *Candida*. *Agric.*  
28 *Biol. Chem.* 45 (2), 475-479.
- 29 [10] Strelko, C. L., Lu, W., Dufort, F. J., Seyfried, T. N., Chiles, T. C., Rabinowitz, J. D.,  
30 and Roberts, M. F. (2011) Itaconic acid is a mammalian metabolite induced  
31 during macrophage activation. *J. Am. Chem. Soc.* 133 (41), 16386-16389.
- 32 [11] Cordes, T., Michelucci, A., and Hiller, K. (2015) Itaconic acid: the surprising role  
33 of an industrial compound as a mammalian antimicrobial metabolite. *Annu.*  
34 *Rev. Nutr.* 35, 451-473.
- 35 [12] Geiser, E., Przybilla, S. K., Friedrich, A., Buckel, W., Wierckx, N., Blank, L. M., and  
36 Bölker, M. (2016) *Ustilago maydis* produces itaconic acid via the unusual  
37 intermediate *trans*-aconitate. *Microb. Biotechnol.* 9 (1), 116-126.
- 38 [13] Li, A., van Luijk, N., Ter Beek, M., Caspers, M., Punt, P., and van der Werf, M.  
39 (2011) A clone-based transcriptomics approach for the identification of genes  
40 relevant for itaconic acid production in *Aspergillus*. *Fungal Genet. Biol.* 48 (6),  
41 602-611.

- 1  
2  
3 1 [14] Kuenz, A., Gallenmüller, Y., Willke, T., and Vorlop, K.-D. (2012) Microbial  
4 2 production of itaconic acid: developing a stable platform for high product  
5 3 concentrations. *Appl. Microbiol. Biotechnol.* 96 (5), 1209-1216.  
6  
7 4 [15] Hevekerl, A., Kuenz, A., and Vorlop, K.-D. (2014) Filamentous fungi in microtiter  
8 5 plates—an easy way to optimize itaconic acid production with *Aspergillus*  
9 6 *terreus*. *Appl. Microbiol. Biotechnol.* 98 (16), 6983-6989.  
10 7 [16] Krull, S., Hevekerl, A., Kuenz, A., and Prüße, U. (2017) Process development of  
11 8 itaconic acid production by a natural wild type strain of *Aspergillus terreus* to  
12 9 reach industrially relevant final titers. *Appl. Microbiol. Biotechnol.* 101 (10),  
13 10 4063-4072.  
14  
15 11 [17] Kanamasa, S., Dwiarti, L., Okabe, M., and Park, E. Y. (2008) Cloning and  
16 12 functional characterization of the cis-aconitic acid decarboxylase (CAD) gene  
17 13 from *Aspergillus terreus*. *Appl. Microbiol. Biotechnol.* 80 (2), 223-229.  
18  
19 14 [18] Levinson, W. E., Kurtzman, C. P., and Kuo, T. M. (2006) Production of itaconic  
20 15 acid by *Pseudozyma antarctica* NRRL Y-7808 under nitrogen-limited growth  
21 16 conditions. *Enzyme Microb. Technol.* 39 (4), 824-827.  
22  
23 17 [19] Otten, A., Brocker, M., and Bott, M. (2015) Metabolic engineering of  
24 18 *Corynebacterium glutamicum* for the production of itaconate. *Metab. Eng.* 30,  
25 19 156-165.  
26  
27 20 [20] Harder, B.-J., Bettenbrock, K., and Klamt, S. (2016) Model-based metabolic  
28 21 engineering enables high yield itaconic acid production by *Escherichia coli*.  
29 22 *Metab. Eng.* 38, 29-37.  
30  
31 23 [21] Blazeck, J., Miller, J., Pan, A., Gengler, J., Holden, C., Jamoussi, M., and Alper, H.  
32 24 S. (2014) Metabolic engineering of *Saccharomyces cerevisiae* for itaconic acid  
33 25 production. *Appl. Microbiol. Biotechnol.* 98 (19), 8155-8164.  
34  
35 26 [22] Blazeck, J., Hill, A., Jamoussi, M., Pan, A., Miller, J., and Alper, H. S. (2015)  
36 27 Metabolic engineering of *Yarrowia lipolytica* for itaconic acid production.  
37 28 *Metab. Eng.* 32, 66-73.  
38  
39 29 [23] Guevarra, E. D., and Tabuchi, T. (1990) Accumulation of itaconic, 2-  
40 30 hydroxyparaconic, itatartaric, and malic acids by strains of the genus *Ustilago*.  
41 31 *Agric. Biol. Chem.* 54 (9), 2353-2358.  
42  
43 32 [24] Zambanini, T., Tehrani, H. H., Geiser, E., Merker, D., Schleese, S., Krabbe, J.,  
44 33 Buescher, J. M., Meurer, G., Wierckx, N., and Blank, L. M. (2017) Efficient  
45 34 itaconic acid production from glycerol with *Ustilago vetiveriae* TZ1. *Biotechnol.*  
46 35 *Biofuels* 10 (1), 131.  
47  
48 36 [25] Rogers, J. K., Taylor, N. D., and Church, G. M. (2016) Biosensor-based  
49 37 engineering of biosynthetic pathways. *Curr. Opin. Biotechnol.* 42, 84-91.  
50  
51 38 [26] Rogers, J. K., Guzman, C. D., Taylor, N. D., Raman, S., Anderson, K., and Church,  
52 39 G. M. (2015) Synthetic biosensors for precise gene control and real-time  
53 40 monitoring of metabolites. *Nucleic Acids Res.* 43 (15), 7648-7660.  
54  
55 41 [27] Raman, S., Rogers, J. K., Taylor, N. D., and Church, G. M. (2014) Evolution-guided  
56 42 optimization of biosynthetic pathways. *Proc. Natl. Acad. Sci. U.S.A.* 111 (50),  
57 43 17803-17808.  
58  
59  
60

- 1  
2  
3 1 [28] Rogers, J. K., and Church, G. M. (2016) Genetically encoded sensors enable real-  
4 2 time observation of metabolite production. *Proc. Natl. Acad. Sci. U.S.A.* *113*  
5 3 (9), 2388-2393.
- 6  
7 4 [29] Klement, T., and Büchs, J. (2013) Itaconic acid—a biotechnological process in  
8 5 change. *Bioresour. Technol.* *135*, 422-431.
- 9  
10 6 [30] Cooper, R., and Kornberg, H. (1964) The utilization of itaconate by *Pseudomonas*  
11 7 sp. *Biochem. J.* *91* (1), 82.
- 12  
13 8 [31] Martin, W. R., Frigan, F., and Bergman, E. H. (1961) Noninductive metabolism of  
14 9 itaconic acid by *Pseudomonas* and *Salmonella* species. *J. Bacteriol.* *82* (6), 905-  
15 10 908.
- 16  
17 11 [32] Sasikaran, J., Ziemski, M., Zadora, P. K., Fleig, A., and Berg, I. A. (2014) Bacterial  
18 12 itaconate degradation promotes pathogenicity. *Nat. Chem. Biol.* *10* (5), 371-  
19 13 377.
- 20  
21 14 [33] Shi, L., Adkins, J. N., Coleman, J. R., Schepmoes, A. A., Dohnkova, A., Mottaz, H.  
22 15 M., Norbeck, A. D., Purvine, S. O., Manes, N. P., and Smallwood, H. S. (2006)  
23 16 Proteomic analysis of *Salmonella enterica* serovar Typhimurium isolated from  
24 17 RAW 264.7 macrophages: identification of a novel protein that contributes to  
25 18 the replication of serovar Typhimurium inside macrophages. *J. Biol. Chem.* *281*  
26 19 (39), 29131-29140.
- 27  
28 20 [34] Michelucci, A., Cordes, T., Ghelfi, J., Pailot, A., Reiling, N., Goldmann, O., Binz, T.,  
29 21 Wegner, A., Tallam, A., and Rausell, A. (2013) Immune-responsive gene 1  
30 22 protein links metabolism to immunity by catalyzing itaconic acid production.  
31 23 *Proc. Natl. Acad. Sci. U.S.A.* *110* (19), 7820-7825.
- 32  
33 24 [35] Oliver, P., Peralta-Gil, M., Tabche, M.-L., and Merino, E. (2016) Molecular and  
34 25 structural considerations of TF-DNA binding for the generation of biologically  
35 26 meaningful and accurate phylogenetic footprinting analysis: the LysR-type  
36 27 transcriptional regulator family as a study model. *BMC Genomics* *17* (1), 686.
- 37  
38 28 [36] Hanko, E. K. R., Minton, N. P., and Malys, N. (2017) Characterisation of a 3-  
39 29 hydroxypropionic acid-inducible system from *Pseudomonas putida* for  
40 30 orthogonal gene expression control in *Escherichia coli* and *Cupriavidus*  
41 31 *necator*. *Sci. Rep.* *7* (1), 1724.
- 42  
43 32 [37] Pfeiffer, D., and Jendrossek, D. (2011) Interaction between poly (3-  
44 33 hydroxybutyrate) granule-associated proteins as revealed by two-hybrid  
45 34 analysis and identification of a new phasin in *Ralstonia eutropha* H16.  
46 35 *Microbiology* *157* (10), 2795-2807.
- 47  
48 36 [38] Campbell, R. E., Tour, O., Palmer, A. E., Steinbach, P. A., Baird, G. S., Zacharias, D.  
49 37 A., and Tsien, R. Y. (2002) A monomeric red fluorescent protein. *Proc. Natl.*  
50 38 *Acad. Sci. U.S.A.* *99* (12), 7877-7882.
- 51  
52 39 [39] Blazeck, J., and Alper, H. S. (2013) Promoter engineering: recent advances in  
53 40 controlling transcription at the most fundamental level. *Biotechnol. J.* *8* (1),  
54 41 46-58.
- 55  
56 42 [40] Taylor, N. D., Garruss, A. S., Moretti, R., Chan, S., Arbing, M. A., Cascio, D.,  
57 43 Rogers, J. K., Isaacs, F. J., Kosuri, S., and Baker, D. (2016) Engineering an

- 1  
2  
3 1 allosteric transcription factor to respond to new ligands. *Nat. Methods* 13 (2),  
4 2 177-183.  
5 3 [41] Mannan, A. A., Liu, D., Zhang, F., and Oyarzún, D. A. (2017) Fundamental design  
6 4 principles for transcription-factor-based metabolite biosensors. *ACS Synth.*  
7 5 *Biol.* 6 (10), 1851-1859.  
8 6 [42] Vuoristo, K. S., Mars, A. E., Sangra, J. V., Springer, J., Eggink, G., Sanders, J. P.,  
9 7 and Weusthuis, R. A. (2015) Metabolic engineering of itaconate production in  
10 8 *Escherichia coli*. *Appl. Microbiol. Biotechnol.* 99 (1), 221-228.  
11 9 [43] Bi, C., Su, P., Müller, J., Yeh, Y.-C., Chhabra, S. R., Beller, H. R., Singer, S. W., and  
12 10 Hillson, N. J. (2013) Development of a broad-host synthetic biology toolbox for  
13 11 *Ralstonia eutropha* and its application to engineering hydrocarbon biofuel  
14 12 production. *Microb. Cell Fact.* 12 (1), 1-10.  
15 13 [44] Sambrook, J., and Russell, D. W. (2001) *Molecular Cloning: A Laboratory Manual*,  
16 14 3rd ed., Cold Spring Harbor Laboratory Press, New York.  
17 15 [45] Jensen, K. F. (1993) The *Escherichia coli* K-12 "wild types" W3110 and MG1655  
18 16 have an *rph* frameshift mutation that leads to pyrimidine starvation due to  
19 17 low *pyrE* expression levels. *J. Bacteriol.* 175 (11), 3401-3407.  
20 18 [46] Schlegel, H., Kaltwasser, H., and Gottschalk, G. (1961) Ein Submersverfahren zur  
21 19 Kultur wasserstoffoxydierender Bakterien: Wachstumsphysiologische  
22 20 Untersuchungen. *Archiv für Mikrobiologie* 38 (3), 209-222.  
23 21 [47] Ausubel, F. M., Brent, R., Kingston, R. E., Moore, D. D., Seidman, J. G., and Struhl,  
24 22 K. e. (2003) *Current Protocols in Molecular Biology*, John Wiley & Sons.  
25 23 [48] Duportet, X., Aggio, R. B. M., Carneiro, S., and Villas-Bôas, S. G. (2012) The  
26 24 biological interpretation of metabolomic data can be misled by the extraction  
27 25 method used. *Metabolomics* 8 (3), 410-421.  
28 26 [49] Martinez-Salas, E., Martin, J., and Vicente, M. (1981) Relationship of *Escherichia*  
29 27 *coli* density to growth rate and cell age. *J. Bacteriol.* 147 (1), 97-100.  
30  
31  
32  
33  
34  
35  
36  
37  
38  
39  
40  
41  
42  
43  
44  
45  
46  
47  
48  
49  
50  
51  
52  
53  
54  
55  
56  
57  
58  
59  
60